Supported Ni and Pt-Ni Nanoparticles by Supercritical Deposition

Ramazan Oğuz Canıaz[1] and Can Erkey[2,*]

[1]Turkish Petroleum Refineries Corporation, Izmit 41780Turkey
[2]Department of Chemical and Biological Engineering, Koc University, 34450 Sarıyer, Istanbul, Turkey
Phone: +90 (212) 338 18 66, Fax: +90 (212) 338 15 48,
e-mail:cerkey@ku.edu.tr

Monometallic nickel and bimetallic platinum-nickel nanoparticles were deposited on γ-Al_2O_3, Vulcan XC72R and carbon aerogel (CA) supports by supercritical carbon dioxide ($scCO_2$) deposition (SCD). Characterization of the samples was carried out by BET, TPD, XRD, TEM, and EDXS. Nickel acetylacetonate ($Ni(acac)_2$) was adsorbed on the supports from $scCO_2$ solutions. The adsorbed Ni precursor was reduced to nickel nanoparticles by heat treatment under hydrogen. The resulting nanoparticles had an average size of 6 nm. Bimetallic Pt-Ni nanoparticles were synthesized by a two-step procedure termed sequential deposition. First, Pt nanoparticles were deposited on the supports by adsorption of platinum cyclooctadiene dimethyl $Pt(cod)(me)_2$ from $scCO_2$ solution followed by reduction of the adsorbed precursor to Pt by heat treatment at 200 ^oC under flowing nitrogen. Subsequently, $Ni(acac)_2$ was adsorbed on Pt/support from $scCO_2$. The adsorbed Ni precursor was then reduced to Ni by heat treatment under hydrogen. Spherical nanoalloys of Pt-Ni nanoparticles with uniform sizes of ~3nm were obtained over Vulcan XC 72R, and Pt-Ni nanoparticles with uniform sizes of ~1nm were successfully synthesized over carbon aerogel. As for the alumina support, supported Pt-Ni nanoparticles of ~3 nm in size were obtained. The small composition variations in EDXS measurements indicated a uniform distribution of the bimetallic nanoparticles. The effect of the order of sequential deposition of Pt and Ni on both morphology and activity of the synthesized materials were also investigated. It was found that the formation of Ni nanoparticles occurs on the previously deposited Pt islands resulting in bimetallic spherical nanoparticles having homogeneous chemical compositions with no phase separation when Pt deposition is carried out first and this is followed by Ni deposition. Interestingly, the size of the bimetallic nanoparticles was found to be smaller than the size of the monometallic Ni. However, pure Ni agglomerates were observed on TEM images when Ni deposition is achieved first and this was followed by Pt addition. Cyclic voltammograms of the carbon supported catalysts were also determined. Bimetallic nanocatalysts showed a higher activity than the monometallic nanocatalysts. Among the bimetallic nanocatalysts, higher activity was obtained when Pt deposition was carried out first.

INTRODUCTION

Supported monometallic Ni and bimetallic Pt-Ni catalysts are known to catalyze a wide variety of reactions. For example, γ-alumina supported Ni nanoparticles are used extensively for reforming, γ-alumina supported bimetallic PtNi nanoparticles are used for reforming, hydrogenation and hydroisomerization (see Figure 1), and carbon supported bimetallic PtNi are promising candidates for oxidation and reduction reactions in fuel cells. In addition to reforming and hydrogenation applications of refineries, if acidity of the support is increased with zeolite addition and Pt is replaced with other metals such as tungsten and molybdenum for poisoning issues, then supported Ni catalysts can be used for hydrocracking of heavy vacuum gas oil which is generally the most profitable unit of a refinery [1-3].

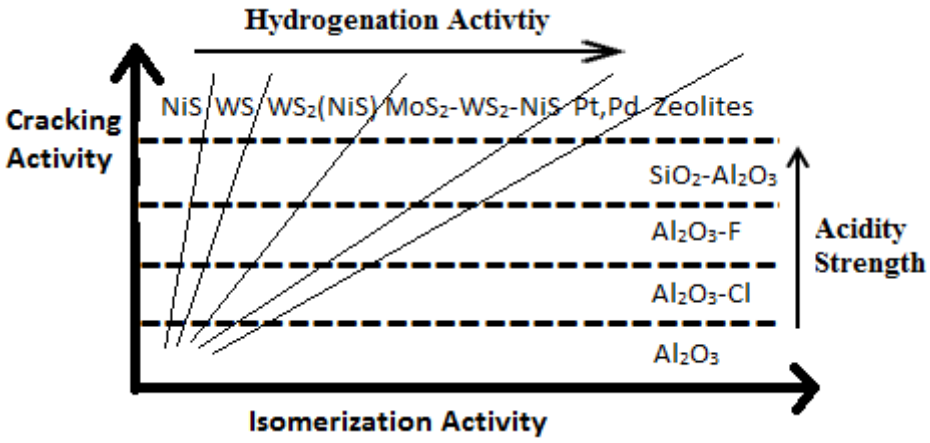

Figure 1. Hydrogenation and cracking activity of the hydrocracking catalysts as a function of metal type and support's acidity [4].

The size, shape, size distribution, loading, and impregnation sequence are important to tune the activity and selectivity of the synthesized catalysts and these parameters depend on the preparation techniques. As compared to the techniques such as wet / dry impregnation, co-precipitation, and sol-gel, SCD is a relatively new technique for the preparation of supported metal nanoparticles [5]. A SCF has properties intermediate between a liquid and a gas. It is capable of dissolving solutes like a liquid and exhibits almost no surface tension with low viscosity that enables the good penetration of the dissolved molecules into the small pores. The liquid solvents usually are not favorable for the wetting of very small pores which results in low utilization of the support for metal deposition Another advantage of a SCF is the sensitivity of its density to the changes in temperature and pressure which makes it possible to manipulate the solvent properties during processing [5, 6].

In addition to the metal pairs deposited and the deposition techniques employed, the support material also has a notable influence on the activity of the catalysts [7-9]. Pore size, pore volume, surface area, acidity and conductivity are the key factors that determine the effect of the support on the activity and selectivity of the catalyst.

In this study, SCD was used to synthesize supported monometallic Ni and bimetallic Pt-Ni nanoparticles. Commercially available supports of γ-alumina and Vulcan XC72R as well as carbon aerogels prepared in our laboratory were used as supports. Bimetallic nanoparticles were synthesized by the technique called sequential deposition. The effects of support, metal loading, impregnation and reduction conditions on the particle size, particle size distribution and activity were investigated.

Prepared catalysts were characterized by XRD, TEM, and EDX. The electrochemical activity of the synthesized catalysts was determined by cyclic voltammetry.

MATERIALS AND METHODS

Materials

Dimethyl (cyclooctadiene) platinum (II) ($PtMe_2COD$) (99.9%) and Bis(2,4-pentanedionato)nickel(II) ($Ni(acac)_2$) were purchased from Strem Chemicals. Vulcan XC 72R carbon black powder was obtained from Cabot International. Spherical γ-alumina particles

with a diameter of 1.6 mm were purchased from Saint-Gobain NorPro, Inc. For the carbon aerogel preparation, resorcinol (99%), formaldehyde (37%), and sodium carbonate (99.99%) were bought from Aldrich and used without further purification. All of the supports used in this study were dried in the oven at 150 ^{o}C for 4 hours before use in order to remove the water. Carbon dioxide (99.998%) and nitrogen (99.999%) were purchased from Airgas.

Methods

The supercritical fluid deposition setup is shown in Figure 2. The custom manufactured stainless steel vessel with a 54 ml volume is equipped with two sapphire windows (1 in, id; Sapphire Engineering, Inc.) and each sapphire window is sealed with 2 poly(ether ether ketone) O-rings. In addition, a vent line, a rupture disk assembly (Autoclave Engineers) and T-type thermocouple assembly (Omega Engineering, PX300-7.5KGV) are included in the system.

For each experiment, a known amount of support was placed in a bag made from filter paper and inserted into the reaction vessel together with the organometallic compound. The system was heated with a circulating heater and after thermal equilibrium was reached, the system was filled with CO_2 by a syringe pump. Deposition experiments were performed at 4400 psi/60^{o}C and at 3500psi/70^{o}C for Ni and Pt deposition, respectively. To ensure that adsorption equilibrium was reached, the system was let to stay at these conditions for 48 hours. Then the system was depressurized and adsorbed organometallic compounds were converted to metallic nanoparticles at atmospheric pressure under hydrogen and nitrogen flow for Ni and Pt, respectively. For the preparation of bimetallic catalysts, the sequential impregnation method was used. The supported monometallic nanoparticles were treated as a support material for the deposition of second metal and the same procedure was followed. This enabled us to study the effect of impregnation sequence on the structure and activity of the catalysts.

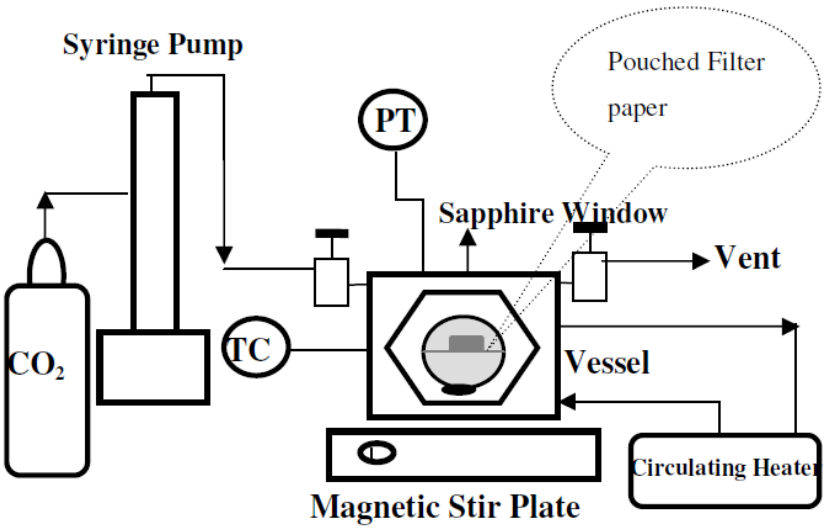

Figure 2. Supercritical Carbon Dioxide Deposition Setup.

Support characterization was done by TPD and BET. XRD measurements were carried out by using Cu Kα source Huber G 670 Imaging Plate in a 2θ range of 5-85º with a step size of 0.01º. The morphology of the prepared catalysts was analyzed by TEM, and the chemical compositions were found by EDXS measurements. Activity tests of the prepared catalysts were done by CV measurements in 0.1 M $HClO_4$ electrolyte solution.

RESULTS

Characterization of the support materials were done by BET and TPD measurements. CA support was found to have a surface area of 747 m^2/g, average pore diameter of 22 nm and pore volume of 4.1 cm^3/g. The Vulcan XC72R was found to have a surface area of 213 m^2/g, pore diameter of 6.4 nm and pore volume of 0.48 cm^3/g. As for γ–alumina support, the surface area of 260 m^2/g, pore diameter of 10 nm and pore volume of 0.83 cm^3/g were determined. TPD result of γ–alumina support is given in Figure 3 showing the amount of the ammonia desorbed from the surface. The acidity of γ-alumina support was found as 0.491 mmol ammonia / g catalyst.

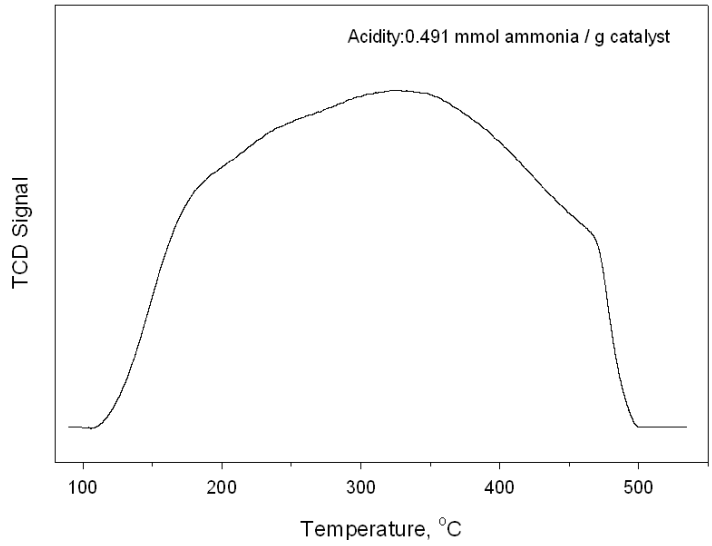

Figure 3. TPD of ammonia results of γ–alumina.

The solubility of $Ni(acac)_2$ was found to be low to obtain high Ni loadings [10]. Therefore a few mL of methanol was introduced as an entrainer. Excess amount of $Ni(acac)_2$ was used to ensure that maximum Ni loadings on all of the supports were obtained.

Maximum nickel loading on γ–alumina was found to be 3%. All the loadings specified in this study are weight percentages. The XRD spectrum for 3%Ni/γ–alumina is given in Figure 4. The detection of the corresponding Ni peaks is hard because of the low loading of the metal, the nanosize of the metal particles, and the interference with polycrystalline alumina peaks. However, deposition of Ni metal nanoparticles was confirmed by TEM images and EDXS results. Small nanoparticles with a size of ~6nm were observed and the chemistry of these particles was analyzed by EDX indicating pure Ni nanoparticles formation.

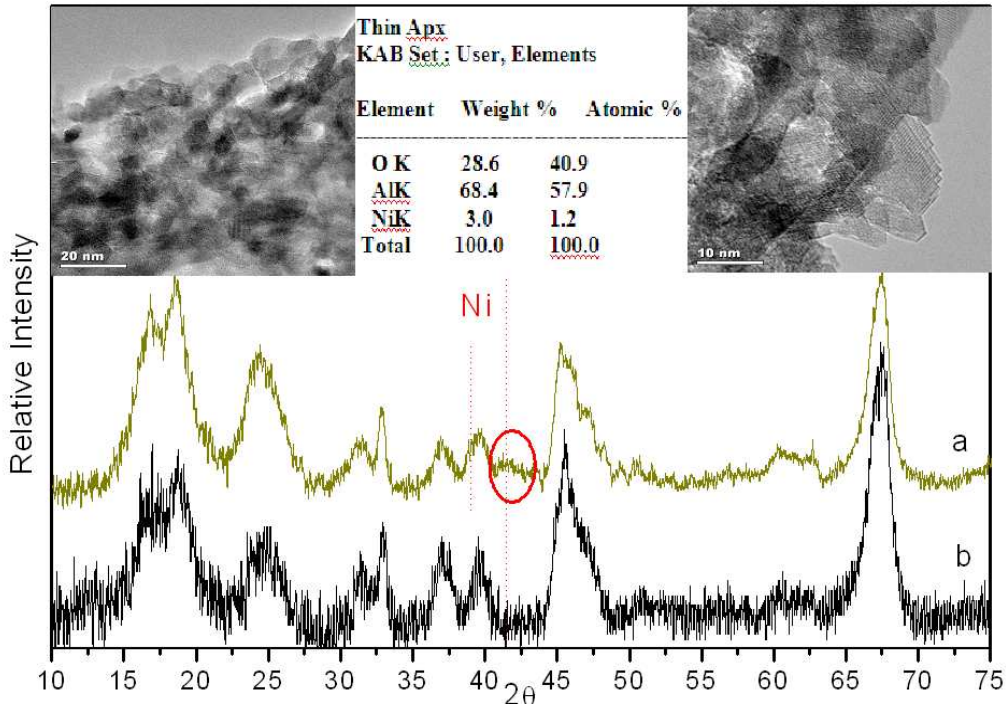

Figure 4. Characterization results of the supported monometallic nickel nanoparticles on γ-alumina. (Top left and top right: TEM images; Top middle: Chemical Composition based on EDX results; XRD spectra a: 3wt% Ni on γ-alumina; XRD spectra b: pure γ-alumina)

To synthesize bimetallic PtNi/γ-alumina, firstly monometallic Pt/γ-alumina was prepared with a loading of 2.5wt% Pt. For similar reasons mentioned above, XRD results of Pt/γ-alumina were found to be inconclusive. Secondly, Pt/γ-alumina was treated as a support material and Ni deposition with a loading of 1.5wt% was achieved. TEM images and EDXS results of PtNi/ γ-alumina nanocatalysts are given in Figure 5. Supported nanoparticles of 1-3nm in size were observed with a narrow particle size distribution. It is interesting to note that size of the bimetallic Pt-Ni nanoparticles is smaller than the size of the monometallic Ni nanoparticles. The particle size distribution and shape of the bimetallic Pt-Ni nanoparticles are similar to the shape and size of the monometallic Pt nanoparticles on γ-alumina prepared by SCD [11]. This supports the argument stating that Ni nanoparticle formations occur with close contact to the Pt islands; therefore, instead of phase separation, bimetallic PtNi nanoparticles with homogeneous chemical compositions were obtained. Bayrakçeken et al studied Pt based bimetallic nanostructures by SCD and found that Pd agglomerate formations can be stabilized if there are pre-existing Pt islands on the surface but phase separation still occurred [12]. The findings of our study, on the other hand, states that Pt and Ni further interact with each other giving small composition variations in EDX measurements indicating no phase separation.

The characterization results suggest that prepared γ-alumina supported bimetallic PtNi nanocatalyst with uniformly distributed metal content at nanosize is a good candidate to be a reforming and hydrogenation catalyst for refinery operations.

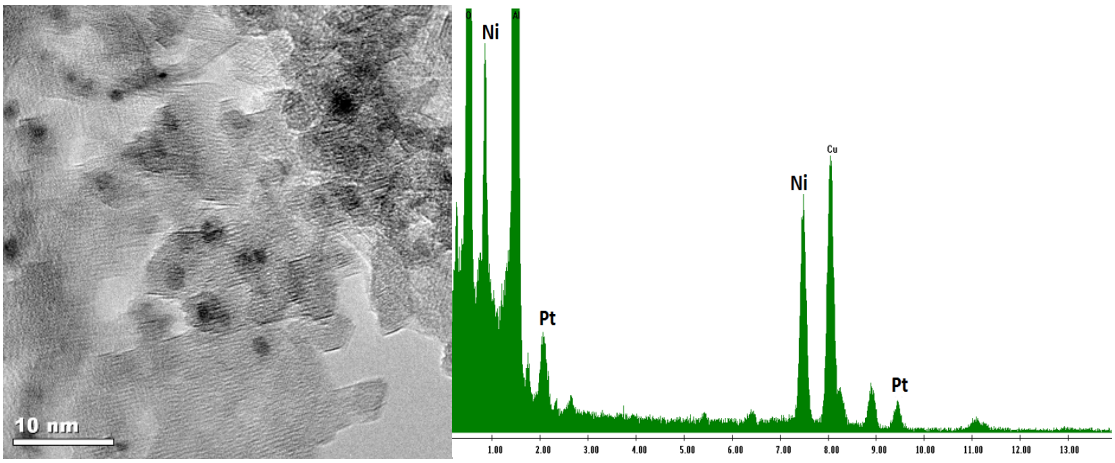

Figure 5. PtNi/ γ-alumina nanocatalysts. TEM image(left) and EDXS spectra (right).

As for the characterization results of nanocatalysts supported by Vulcan XC72R, XRD spectrum of the naked support, Pt deposited support, and PtNi deposited support are given in Figure 6 together with the particle size analysis results and corresponding TEM images. Particle size was calculated using the width of the (111) peak at half maximum. Particle size was observed to increase from 2.1 nm (8 wt% Pt) to 2.8 nm (8 wt% Pt + 2 wt% Ni) after Ni deposition suggesting that Ni metal is not phase separated; instead Ni atoms grow on the previously deposited Pt islands. Information obtained from XRD analysis is volume averaged but TEM information on the other hand is specific to the area focused on the TEM specimen. Therefore calculated particle size of 2.8 nm which is close to the observed value on TEM images (~3 nm) indicates that SCD enables to have narrow particle size distribution.

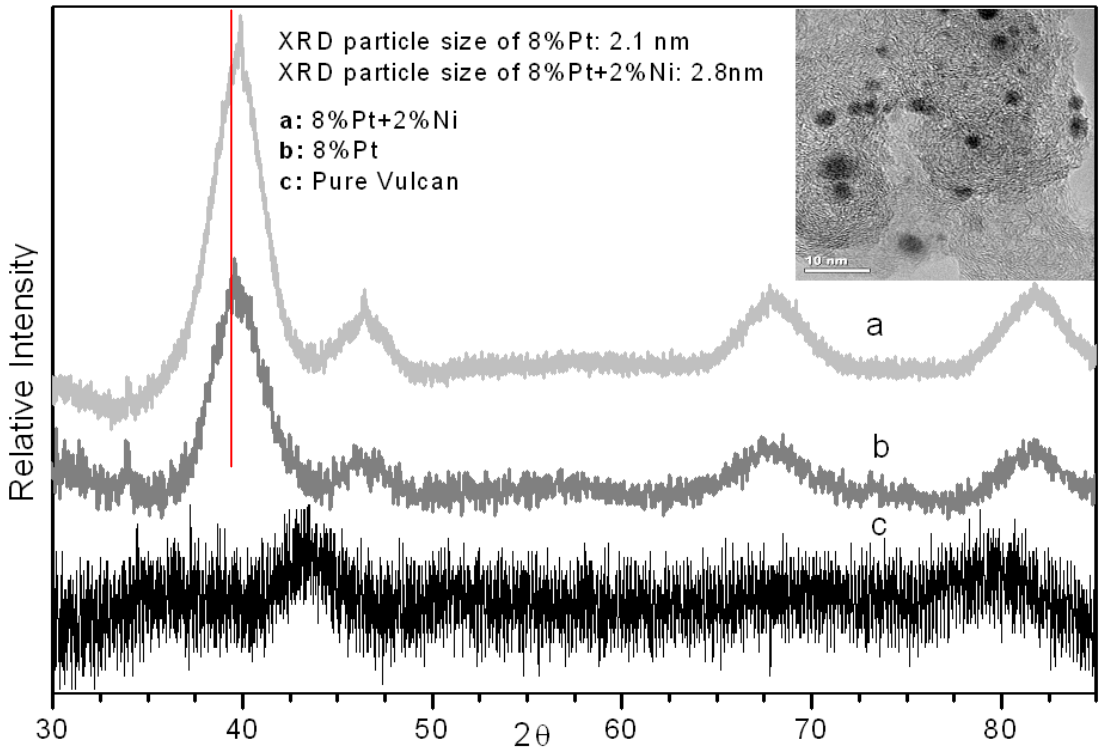

Figure 6. XRD diffractograms of pure Vulcan XC 72R (c), 8 wt%Pt/Vulcan XC 72R (b), (8wt %Pt+2 wt %Ni)/Vulcan XC 72R (a), particle size calculated from (111) peak, and the corresponding TEM image of (8 wt%Pt+2 wt% Ni)/Vulcan XC 72R (top right-scale base is 10nm).

As for the CA support, two types of bimetallic PtNi nanocatalysts were prepared to see the effect of the impregnation sequence on the morphology and activity of the catalysts. The prepared monometallic nanocatalysts were treated as support material for the deposition of the second type of metal. One of them was prepared by Pt deposition first and this was followed by Ni deposition. The second one was prepared by Ni deposition first and this was followed by Pt deposition.

Figure 7 shows TEM images of the first type of bimetallic PtNi. The particle sizes obtained were close to ~1nm. The metal nanoparticles are highlighted with the arrows and the circles. No agglomerate formation was observed on TEM images. Small variation in EDX measurements indicated that there was no phase separation on the surface. Extremely small particle sizes can be attributed to the high available surface area of the CA support. The surface area of the CA support was measured as 747 m^2/g which prevents the metal particles to come together and form bigger agglomerates.

Characterization results of the second type of bimetallic PtNi is given in Figure 8. The Ni metal loading of 3.5 wt% was obtained on CA support and this was followed by 3.6wt% Pt deposition. Interestingly, according to the TEM and EDX results, bimetallic PtNi nanoparticles of ~1-3 nm in size were observed together with bigger and pure Ni nanoparticles of ~10-20 nm in size. No such big particles on the corresponding TEM images of monometallic 3.5wt% Ni/CA was observed (~5nm). Therefore, these bigger particles of pure Ni with a size of ~10-20 nm can possibly be explained by the heat supplied to the catalyst after the adsorption of Pt precursor to obtain Pt nanoparticles. The pre-existing Ni metals gained the mobility and formed bigger particles. This order in sequential impregnation resulted in bimetallic PtNi nanocatalyst with a quite different morphology. Therefore, it is suggested that pre-existing Pt islands stabilized the Ni growth but when Ni deposition was achieved first, the phase separation and agglomerate formation couldn’t be inhibited.

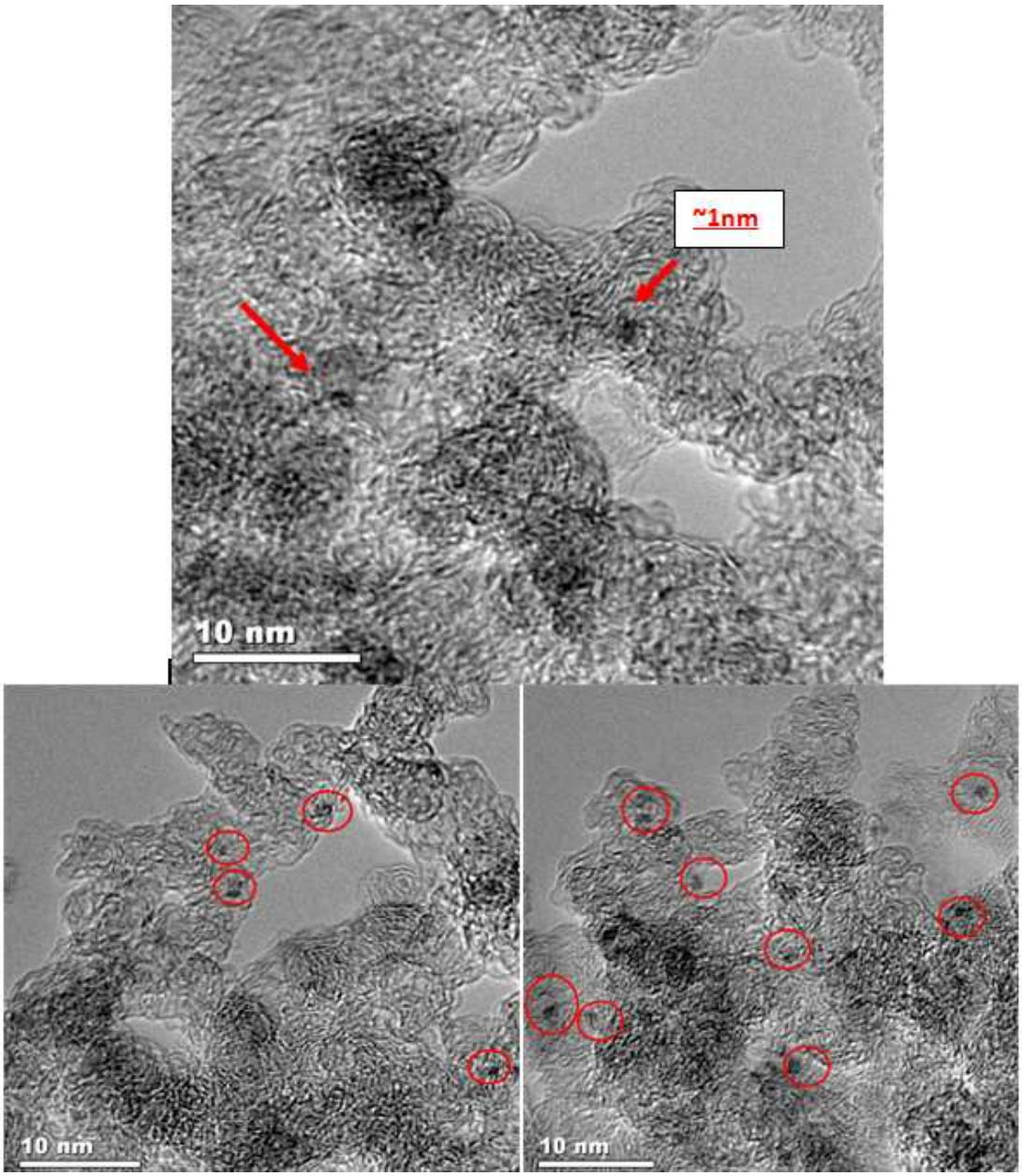

Figure 7. High magnification TEM images of PtNi/CA with the metal loadings of 2.2wt% Pt and 1wt %Ni.

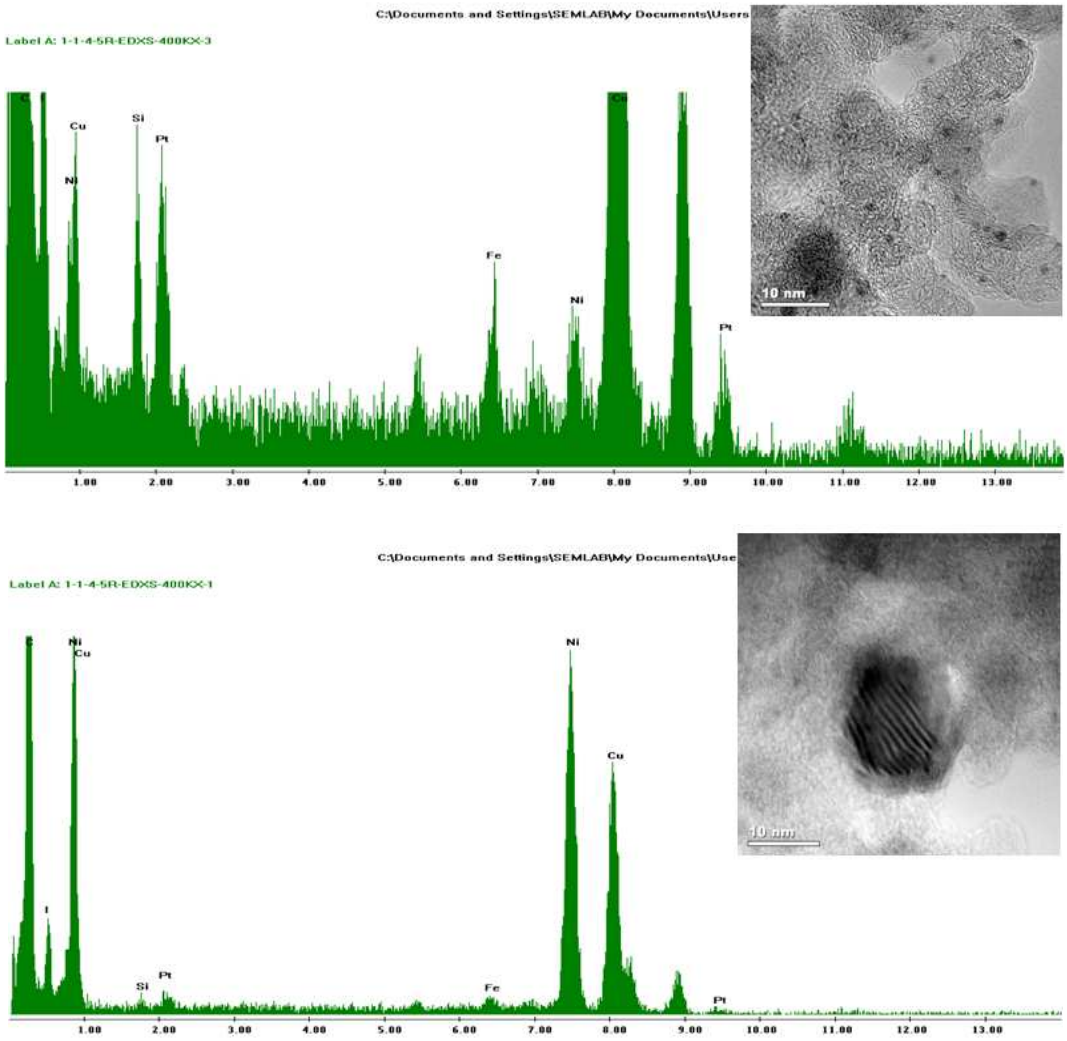

Figure 8. TEM images and the corresponding EDX results of PtNi/CA with the metal loadings of 3.5wt% Ni and 3.6wt %Pt.

The electrochemical activity was determined by CV. As for the activity tests, cyclic voltammograms of HOR and ORR for both of the carbon supported catalysts were collected. Figures 9 and 10 display the cyclic voltammograms of carbon supported monometallic Pt and PtNi nanocatalysts. It is clearly seen that Ni addition improves the ORR activity. These improvements can be explained by the modifications either in the electronic structure or in the geometric structure of the Pt. Alternatively, nickel addition may weaken the bonds between Pt and undesired adsorbates.

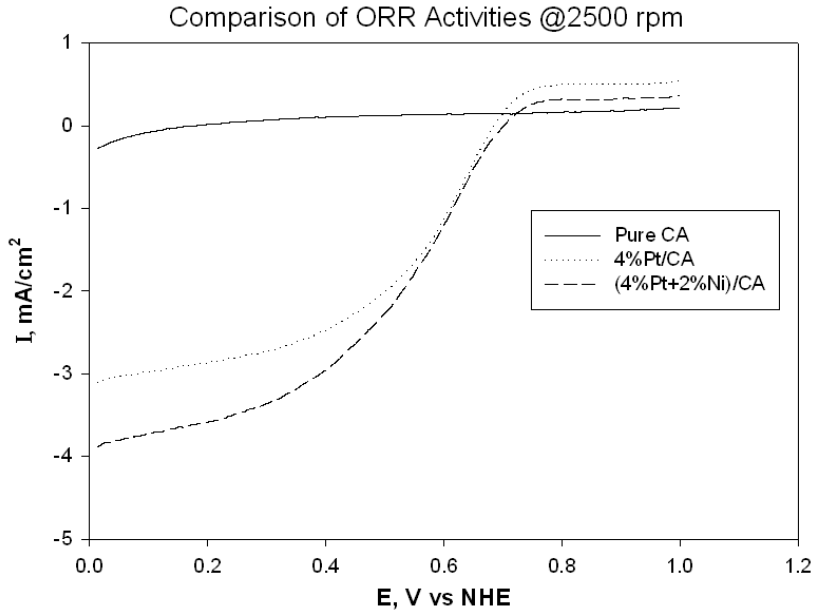

Figure 9. Comparison of the hydrodynamic voltammograms of positive scans of pure CA, (4%Pt)/CA, and (4%Pt + 2%Ni)/CA for O_2 reduction in O_2 saturated 0.1 M $HClO_4$.

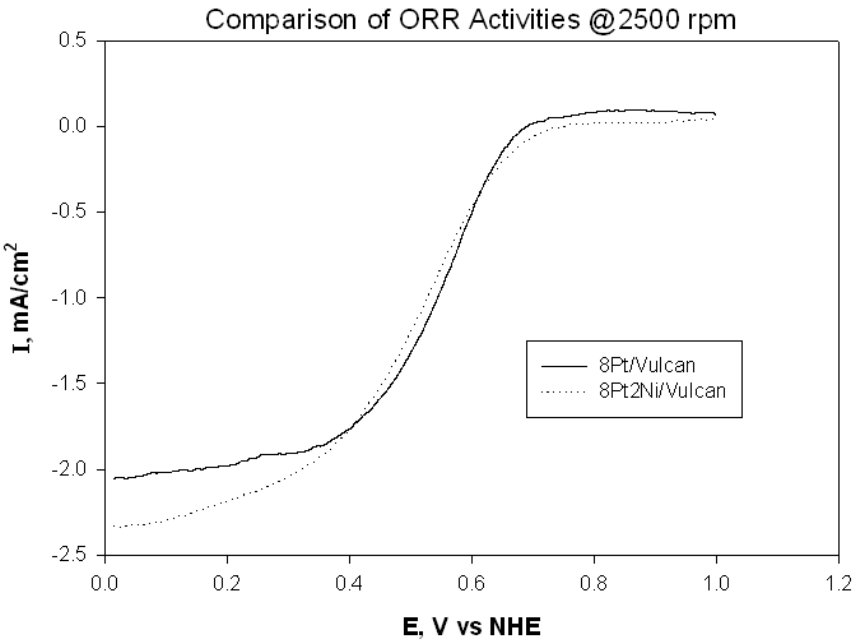

Figure 10. Comparison of the hydrodynamic voltammograms of positive scans of (8%Pt)/Vulcan XC 72R, and (8%Pt+2%Ni)/Vulcan XC 72R for O_2 reduction in O_2 saturated 0.1 M $HClO_4$.

CONCLUSIONS AND FUTURE WORK

Supported monometallic Ni and bimetallic PtNi nanocatalysts with different deposition sequences were prepared on γ-alumina, Vulcan XC72R and CA by SCD. It was found that Ni nanoparticle formation does not occur away from the previously deposited Pt islands which would results in a phase separation. Instead, Pt and Ni metals interacts with each other to form spherical bimetallic nanoparticles having homogeneous chemical compositions. However, Ni agglomerates were observed when Ni deposition was achieved prior to Pt deposition. This suggests that pre-existing Pt inhibits the Ni phase separation and agglomerate formation.

Activity tests were also performed. Higher activities were observed for bimetallic PtNi as compared to the monometallic Pt. As for the effect of impregnation sequence, two types of bimetallic PtNi nanocatalysts were prepared. One with Ni deposition and followed by the Pt addition and the other one with Pt deposition first and followed by Ni incorporation. It was found that the latter exhibits a higher electrochemical activity.

As for the future work, different types of Ni precursors to increase the metal loading will be used. In addition, altering carbonyl precursors to couple nickel not only with platinum but also with tungsten will be studied.

ACKNOWLEDGEMENT

Turkish Petroleum Refineries Corporation (TUPRAS) is greatly acknowledged for its financial support.

NOMENCLATURE

CA:	Carbon Aerogel
$scCO_2$:	Supercritical Carbon Dioxide
SCD:	Supercritical Carbon Dioxide Deposition
BET:	Brunauer Emmett Teller
TPD:	Temperature Programmed Desorption
XRD:	X-ray Diffraction
TEM:	Transmisson Electron Microscopy
EDXS:	Energy Dispersive X-ray Spectroscopy
$Ni(acac)_2$:	Nickel Acetyl Acetonate
$Pt(cod)(me)_2$:	Platinum Cyclooctadiene DiMethyl
CV:	Cyclic Voltammetry
SCF:	Supercritical Fluid
ORR:	Oxygen Reduction Reaction
rpm:	Revolution per minute

REFERENCES:

1. Seo, J.G., M.H. Youn, and I.K. Song, *Hydrogen production by steam reforming of liquefied natural gas (LNG) over nickel catalyst supported on mesoporous alumina prepared by a non-ionic surfactant-templating method.* International Journal of Hydrogen Energy, 2009. **34**(4): p. 1809-1817.
2. Shu, Y., et al., *The effect of impregnation sequence on the hydrogenation activity and selectivity of supported Pt/Ni bimetallic catalysts.* Applied Catalysis A: General, 2008. **339**(2): p. 169-179.
3. Stamenkovic, V.R., et al., *Improved oxygen reduction activity on Pt3Ni(111) via increased surface site availability.* Science, 2007. **315**(5811): p. 493-497.
4. Lin, L., et al., *Research and development of catalytic processes for petroleum and natural gas conversions in the Dalian Institute of Chemical Physics.* Catalysis Today, 1999. **51**(1): p. 59-72.
5. Erkey, C., *Preparation of metallic supported nanoparticles and films using supercritical fluid deposition.* Journal of Supercritical Fluids, 2009. **47**(3): p. 517-522.
6. Zhang, Y. and C. Erkey, *Preparation of supported metallic nanoparticles using supercritical fluids: A review.* Journal of Supercritical Fluids, 2006. **38**(2): p. 252-267.
7. Du, H.D., et al., *Carbon aerogel supported Pt-Ru catalysts for using as the anode of direct methanol fuel cells.* Carbon, 2007. **45**(2): p. 429-435.
8. Rolison, D.R., *Catalytic nanoarchitectures - The importance of nothing and the unimportance of periodicity.* Science, 2003. **299**(5613): p. 1698-1701.
9. Park, G.G., et al., *Pore size effect of the DMFC catalyst supported on porous materials.* International Journal of Hydrogen Energy, 2003. **28**(6): p. 645-650.
10. Aschenbrenner, O., et al., *Solubility of [beta]-diketonates, cyclopentadienyls, and cyclooctadiene complexes with various metals in supercritical carbon dioxide.* The Journal of Supercritical Fluids, 2007. **41**(2): p. 179-186.
11. Haji, S., et al., *Hydrodesulfurization of model diesel using Pt/Al2O3 catalysts prepared by supercritical deposition.* Catalysis Today, 2005. **99**(3-4): p. 365-373.
12. Bayrakceken, A., et al., *PtPd/BP2000 electrocatalysts prepared by sequential supercritical carbon dioxide deposition.* International Journal of Hydrogen Energy, 2010. **35**(21): p. 11669-11680.